Check for updates

ASCE

Spatial Topographic Interpolation for Meandering Channels

Vo Quoc Thanh[1]; Dano Roelvink, Ph.D.[2]; Mick van der Wegen, Ph.D.[3]; Le Xuan Tu[4]; Johan Reyns[5]; and Vo Thi Phuong Linh[6]

Abstract: Bathymetric data plays a major role in obtaining accurate results in hydrodynamic modeling of rivers, estuaries, and coasts. Bathymetries are commonly generated by spatial interpolation methods of data on a model grid. Sparse and limited data will impact the quality of the interpolated bathymetry. This study proposes an efficient spatial interpolation framework for producing a channel bathymetry from sparse, cross-sectional data. The proposed approach consists of three steps: (1) anisotropic bed topography data locations transformed to an orthogonal and smooth grid coordinate system that is aligned with its riverbanks and thalweg; (2) sample data are linearly interpolated to generate river bathymetry; and (3) the generated river bathymetry is converted into its original coordinates. The proposed approach was validated with a high spatial resolution topography of the Tieu estuarine branch. In addition, the proposed approach is compared with other spatial interpolation methods such as ordinary kriging, inverse distance weighting, and kriging with external drift. The proposed approach gives a nearly unbiased topography and a strongly reduced RMSE compared with the other methods. In addition, it accurately reproduces the thalweg. The proposed approach appears to be efficiently applicable for regions with sparse cross-sections. Moreover, river topography generated by the proposed approach is smooth including important morphologic features, making it suitable for two- and three-dimensional hydrodynamic modeling. **DOI: 10.1061/(ASCE)WW.1943-5460.0000582**. © *2020 American Society of Civil Engineers*.

Author keywords: Spatial interpolation; Ordinary kriging; Inverse distance weighting; Kriging with external drift; River topography interpolation; Mekong River.

Introduction

The topography of rivers, estuaries, and coasts plays a crucial role in investigating hydrodynamic processes, water-related contaminant transport, and morphological changes because it strongly influences modeled results (Conner and Tonina 2014). Therefore, topographies should be accurate and detailed. Acquiring detailed bathymetry data is difficult and costly. River bathymetry can be generated by field surveys and remote sensing images (Conner and Tonina 2014; Dilbone et al. 2018; Legleiter 2013). However, remote sensing seems only applicable in clear-flowing and gravel-bed rivers/channels. In cases of muddy channels with high suspended sediment concentration, remote sensing cannot predict accurate river bathymetry due to limited signal penetration. Details and accuracy of river bathymetries by field survey depend on the density of the sampling points acquired. If the sampling points are of low density, they need an interpolating method. River bathymetry interpolation methods are manifold, such as original spatial or controlling-directional interpolations (Bailly du Bois 2011; Carter and Shankar 1997; Caviedes-Voullième et al. 2014; Chen and Liu 2017; Conner and Tonina 2014; Goff and Nordfjord 2004; Hilton et al. 2019; Lai et al. 2018; Legleiter and Kyriakidis 2008; Lin and Chen 2004; Merwade 2009; Merwade et al. 2008; Sear and Milne 2000; Zhang et al. 2016).

River bathymetries in 1D models are represented by cross-sectional data. Distances between cross-sections are usually long. For instance, cross-sections of the 1D ISIS model for the Mekong Delta have distance intervals ranging from 500 to 3,000 m. However, a 2D model of the Mekong River has a grid resolution of 300–600 m (Thanh et al. 2017, 2019). Therefore, the cross-section data is insufficient for the 2D model and requires a spatial interpolation method. There are a number of spatial interpolation methods particularly suitable for river bathymetries, such as linear, inverse distance weighting (IDW), and some kriging methods. These methods are efficiently applied for isotropic data. However, river bathymetry data is strongly influenced by river flows, so it has a certain longitudinal trend. If applications of these interpolation methods do not take into account known spatial trends, they may generate inaccurate river topography (Merwade 2009). Therefore, eliminating longitudinal trends of river bathymetry before applying interpolation methods would give a better prediction. The spatial trends of bathymetric data can be excluded by some approaches, such as converting the data into river-aligned coordinates or forcing metrics. Rivest et al. (2008) conducted a study for obtaining better predictions by converting testing data from the Cartesian grid into the natural coordinates of flow. This improves accuracy of kriging

[1]Ph.D. Fellow, Dept. of Water Science and Engineering, IHE Delft, Netherlands; Faculty of Civil Engineering and Geosciences, Delft Univ. of Technology, Netherlands; Lecturer, College of Environment and Natural Resources, Can Tho Univ., Can Tho, Vietnam (corresponding author). ORCID: https://orcid.org/0000-0001-5940-1798. Email: t.vo@un-ihe.org

[2]Professor, Dept. of Water Science and Engineering, IHE Delft, Netherlands; Faculty of Civil Engineering and Geosciences, Delft Univ. of Technology, Netherlands; Deltares, Delft, Netherlands. Email: d.roelvink@un-ihe.org

[3]Associate Professor, Dept. of Water Science and Engineering, IHE Delft, Netherlands; Deltares, Delft, Netherlands. Email: m.vanderwegen@un-ihe.org

[4]Researcher, Southern Institute of Water Resources Research, Ho Chi Minh, Vietnam. Email: xuantutl@gmail.com

[5]Lecturer/Researcher, Dept. of Water Science and Engineering, IHE Delft, Netherlands; Deltares, Delft, Netherlands. Email: j.reyns@un-ihe.org

[6]Lecturer, College of Environment and Natural Resources, Can Tho Univ., Can Tho, Vietnam. Email: vtplinh@ctu.edu.vn

Note. This manuscript was submitted on March 26, 2019; approved on January 17, 2020; published online on May 19, 2020. Discussion period open until October 19, 2020; separate discussions must be submitted for individual papers. This paper is part of the ***Journal of Waterway, Port, Coastal, and Ocean Engineering***, © ASCE, ISSN 0733-950X.

J. Waterway, Port, Coastal, Ocean Eng., 2020, 146(5): 04020024

methods. Legleiter and Kyriakidis (2008) introduced a geostatistical framework to predict river topography. The framework includes steps for (1) transformation of data into channel-centered coordinates and (2) estimating riverbed elevations. Some kriging methods were applied to estimate the bed elevations, including universal kriging, ordinary kriging with breaklines, kriging with an external drift in which a simple trend is considered based on the relationship between planform and cross-section asymmetry. Merwade (2009) applied a similar framework. First, locations of bathymetric sample points are converted to *sn* coordinates based on centerlines. Then the interpolation methods of IDW, regularized spline, spline with tension, topogrid, natural neighbor (NN), ordinary kriging (OK), and OK with anisotropy were applied for six river reaches. They conclude that it is difficult to determine the best interpolation method due to different sampling densities and distribution. The best interpolators are changed depending on characteristics of sampling data (different river reaches). Zhang et al. (2016) developed an interpolation method, called shortest temporal distance. This method will reduce effects of data anisotropy by using temporal distances metrics. Their method is validated and compared to UK and IDW. In addition, Chen and Liu (2017) compared the three methods of linear interpolation, IDW, and NN in resampling cross-sections. Their finding show that the linear interpolation is a good method which is able to maintain morphologic features in meandering rivers. In summary, a general and common approach for generating river bathymetry excludes effects of data anisotropy and then applies a spatial interpolation method. A common way to diminish anisotropic effects is to convert to centerline coordinates (Goff and Nordfjord 2004; Legleiter and Kyriakidis 2008; Merwade 2009).

The accuracy of an interpolated bathymetry greatly depends on the density and spatial distribution of the sampling data (Merwade 2009). Studies by Legleiter and Kyriakidis (2008) and Zhang et al. (2016) are based on high-resolution data (7 and 50 m, respectively) while Merwade (2009) used separated data occupying 70% of the total samples for interpolation. However, in cases with limited and sparse data such as the Mekong River, Vietnam, this interpolation framework should be modified. The most common 2D river topography of the Mekong River, Vietnam, is derived from cross-sectional data from 1D hydrodynamic models (Dung et al. 2011; Manh et al. 2014; Tran et al. 2018; Triet et al. 2017; Van et al. 2012; Wassmann et al. 2004). Cross-sectional data from these 1D models is sparse, with cross-section spacing at 500–3,000 m.

This study aims to propose an efficient spatial interpolation framework, called anisotropy-removed interpolation method (AR), for generating river and estuarine bed topography from sparse cross-sections. The framework was implemented by three steps: (1) anisotropic bed topography data locations transformed to a channel-fitted coordinate based on riverbanks and thalweg; (2) sample data linearly interpolated to generate bed topography; and (3) the generated river bathymetry is converted into its original coordinates. The testing data is the river topography of the Tieu estuarine branch in the Mekong Delta. The cross-sections used for interpolation are extracted from a high spatial resolution of around 50 m. Distances between these cross-sections range from 500 to 2,000 m. A fine and smooth 2D grid that aligns the river reach is generated based on the riverbanks and the thalweg instead of the centerline between two banks. This step excludes anisotropic effects and adds to the generation of a continuous meandering thalweg. Next the linear interpolation method is used to produce a smooth riverbed surface. Performance of this framework is validated and presented by statistical indices of coefficient of correlation, mean error, and root mean square error in comparison with some commonly used methods of IDW, OK, and kriging with external drift (KED).

Method

Data

The Tieu branch is one of the main Mekong River's branches. The Tieu branch is the smallest branch of the Mekong River in terms of river width and cross-sectional area. Its width and cross-sectional area are 1,100 m and 7,100 m^2, respectively (Nguyen 2008). The river length containing topographic samples is approximately 15 km (Fig. 1). The river width at its mouth is 1,100 m and dramatically decreases landward to around 400 m at the west boundary of the topography.

The topographic samples were collected by the Southern Institute of Water Resources Research, Vietnam in 2010 using an ODOM HYDROTRAC echosounder. Fig 2 presents a histogram

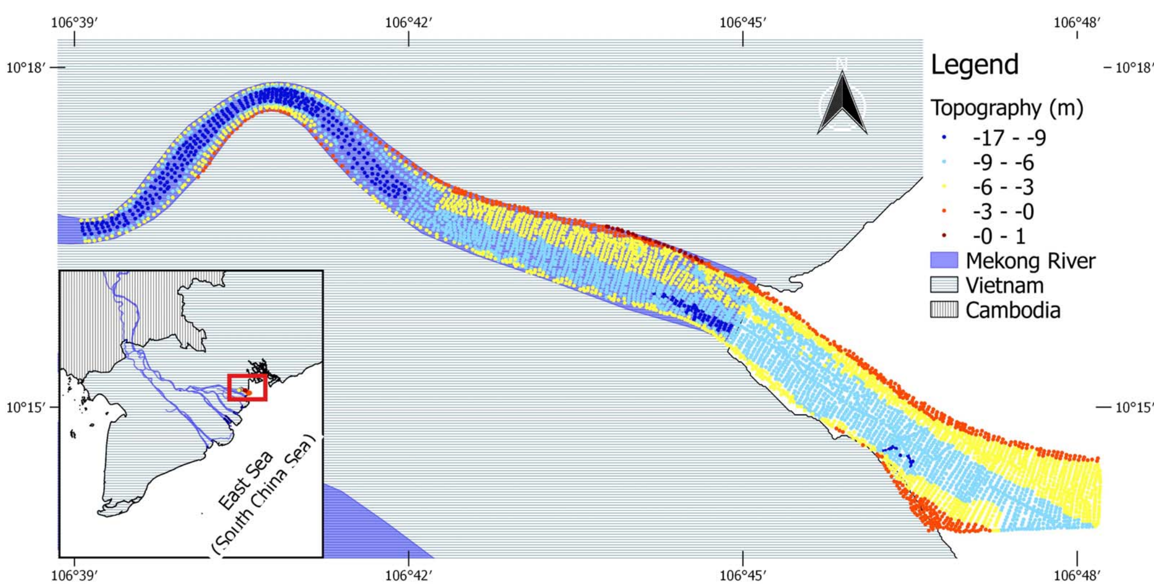

Fig. 1. Location of the Tieu branch and its bed topography collected by the Southern Institute of Water Resources Research, Vietnam in 2010.

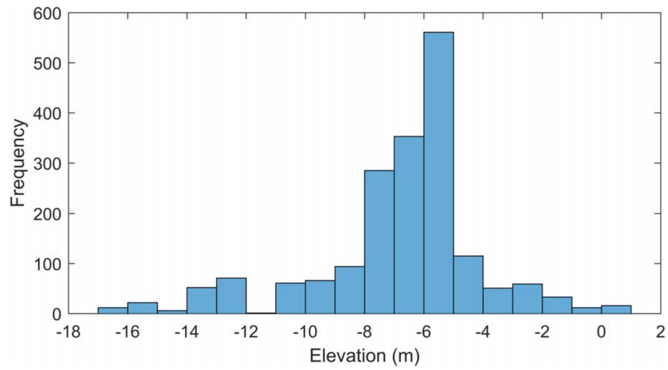

Fig. 2. Histogram of sample of the Tieu branch.

of a sample elevation analyzed from 2,056 samples. The mean and standard deviation of the sample elevation are −6.9 and 2.9 m, respectively. These samples have a relatively uniform distribution in space (Fig. 1). Because the objective of this study is to propose an interpolation approach for sparse and discrete cross-sections, several river cross-sections were extracted at intervals of 500–2,000 m. These intervals are relatively similar to distances between cross-sections in 1D hydrodynamic models for the Mekong Delta, for example, ISIS (Van et al. 2012). The cross-section spacing was still smaller than six times the river width. If it was higher, the interpolated bathymetry would miss the main morphologic features (Conner and Tonina 2014). Distances between the extracted cross-sections depended on the river meandering. The river segments bounded by the extracted cross-sections were as straight as possible. As a result, there are 15 extracted cross-sections, with a total of 186 samples. This number of samples is approximately 9% of the total topographic samples. The remaining samples were used to validate the proposed interpolating approach.

Selected Methods for River Bed Topography Interpolation

There is an increasing amount of interpolation methods applied to river topography estimation (e.g., Bailly du Bois 2011; Carter and Shankar 1997; Caviedes-Voullième et al. 2014; Curtarelli et al. 2015; Merwade 2009; Merwade et al. 2008; Zhang et al. 2016). The most popular methods applied are IDW and OK. However, these methods may be inefficient in cases of sparse and discrete samples. Therefore, we proposed an alternative interpolating approach and compared this to most applied methods, that is, IDW, OK, and KED as described in the following.

Inverse Distance Weighting

IDW is a deterministic interpolation method widely applied in GIS software packages (Li and Heap 2011). The values of nonsampled locations are estimated from the values of several nearby sample points and weights of distances to these points.

The values of nonsampled points ($\hat{z}$) are computed as

$$\hat{z} = \frac{\sum_{i=1}^{n} \left(z_i/d_i^p\right)}{\sum_{i=1}^{n} \left(1/d_i^p\right)} \tag{1}$$

where n = the number of sample points considered; z_i = the value at the i location; d_i = the distance between the estimated point and sample point i; and p = the exponent of a power function. This formula includes two external factors influencing the estimated value, namely the density of the considered sample points and the exponent. In order to apply IDW to create topography, the important factor is the exponent p which accounts for the importance of distance of different sample points. A higher exponent value attaches less importance to longer distance sample points. Commonly used values are $p = 1$ or 2. For the samples used in this study, the exponent value was set to two in the case with a low sampling density.

Ordinary Kriging

OK is the most commonly used kriging method. OK estimates values at nonsampled locations based on the spatial structure of sample points' attribution. Similar to IDW, the attribution of nonsampled points is estimated by neighbor sample points, but with different weights. The weights in the kriging interpolation are statistically specified by the semivariogram. The weight given to each observation depends on the degree of spatial correlation. The semivariogram depicts the spatial autocorrelation of the sample points in accordance with their distances and is calculated as

$$\gamma(h) = \frac{1}{2n} \sum_{k=0}^{n} (z_i - z_{i+h})^2 \tag{2}$$

where z_i = the depth value at the sample i; z_{i+h} = the depth value of a neighbor sample, with distance h from the i location; and n = the number of sample pairs.

All pairs of the sample locations are plotted and a fitting model is used to present the pattern of relationship. For selecting a fitting model, two components need to be considered, encompassing the spatial autocorrelation and the semivariogram model. The former is described by the sample data through certain characteristics which are the range, the sill and the nugget. Semivariogram models are usually described by Exponential, Spherical, Gaussian, Matern, and Linear functions of which the most common type is the Spherical function. In addition, the semivariograms can be defined for a specific direction. However, in the case of meandering, it is really difficult to define a specific direction so the direction is not taken into account in this study.

Kriging with External Drift

Naturally, a channel has a clear trend with aligning riverbanks following the flow direction. Therefore, to consider the effects of the channel direction, an external drift is included in the kriging interpolation, called KED. This dramatically reduces anisotropy effects when taking into account the thalweg of a channel. Distance-to-thalweg is a crucial factor for eliminating effects of anisotropy in interpolating river bathymetry (Wille 2013). In this case, the unknown samples are predicted as in the kriging, but with a different covariance matrix of residuals (Webster and Oliver 2007). In this study, these interpolation methods were implemented in the free software environment of *R*, with the *gstat* geostatistics packages, introduced by Pebesma (2004).

Anisotropy-Removed Interpolation Method

There are numerous studies using 1D models, for example, for the Mekong Delta (Manh et al. 2014; Tran et al. 2018; Triet et al. 2017; Van et al. 2012; Wassmann et al. 2004). The data representing the river topography consist of cross-sections. In order to derive 2D river topography from these cross-sections, an interpolation method is needed.

Isotropic interpolation methods are not suitable because of the anisotropic channel morphology. Merwade et al. (2008) applied isotropic interpolation methods in a transformed coordinate based on the centerline while this study used a transformed coordinate based on the riverbanks and the thalweg. This study introduces an interpolation method specifically for this type of river

J. Waterway, Port, Coastal, Ocean Eng., 2020, 146(5): 04020024

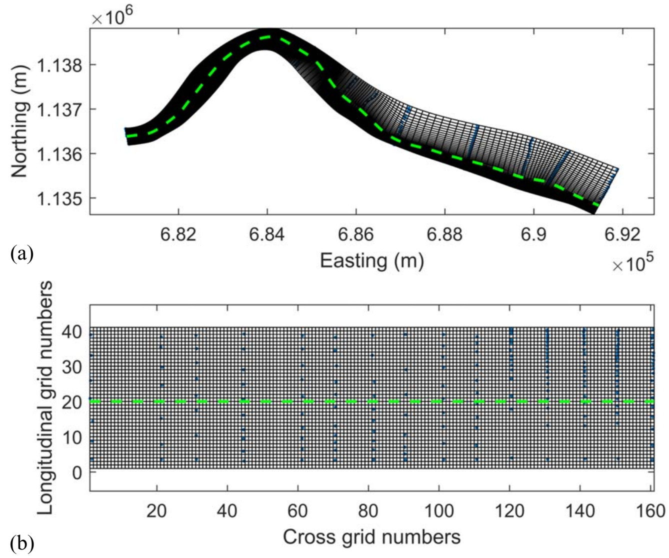

Fig. 3. (a) The grid used in interpolation; and (b) the straightened grid transformed into curvilinear coordinates. The dashed line is the thalweg line and the dots are sampling points for interpolation.

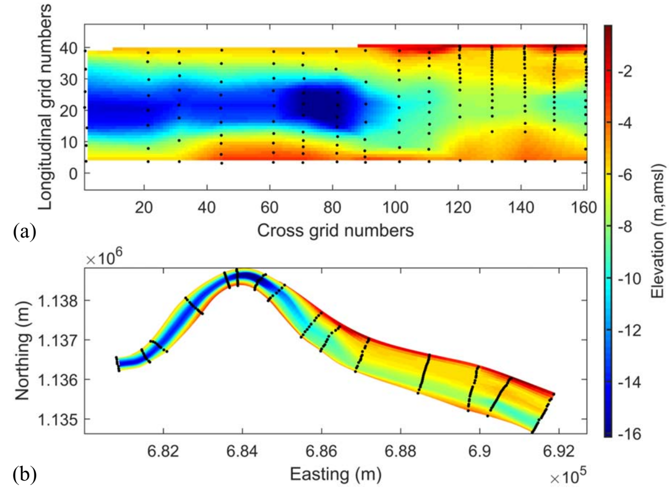

Fig. 4. (a) The estimated bathymetric elevations by the triangle-based interpolation; and (b) these elevations converted to a Cartesian coordination system.

topography data. The interpolation process is illustrated by the following three steps and is implemented in Matlab:

- Step 1: The river segment is presented by an orthogonal and smooth curvilinear grid. The grid is generated based on the riverbanks and the thalweg and it is processed to be orthogonal and smooth in order to accurately represent the river wetted areas. Fig. 3 represents the referenced grid and the samples of cross-sections. The resolution of the grid is fine enough to capture all the samples. This means that the grid sizes should be smaller than the distance between the two closest samples.
- Step 2: The cross-section data in a Cartesian coordination system is transformed into a curvilinear coordinate. Specifically, the grid is straightened in the horizontal and vertical coordinates, representing the longitudinal and cross-directions of the river reach. The curvilinear grid cells are converted to rectangular grid cells (Fig. 3). Simultaneously, the samples are also located in the transformed coordinates. This step is to reduce effects of anisotropy caused by river flows. In the transformed coordinates, the river is presented as a rectangular reach. This general approach was also applied by Merwade (2009). However, in the case of meandering or braided channels, this approach may be insufficient to reproduce continuous thalweg lines. It leads to misleading predictions of the thalweg that generates unrealistic ripples between cross-sections. Therefore, we take the thalweg as a reference for coordinate transformation. The thalweg line, which is the deepest path along the channel, is easily generated based on high-resolution bathymetry. However, it is difficult to identify the thalweg correctly in sparse data channels. It is theoretically defined by the horizontal shapes of channels. For instance, the thalweg would be near the outside bank of bends (Loucks 2008). In these channels with cross-section data, we suggest that the thalweg between their adjacent cross-sections regularly moves along the channels between the thalweg locations on these cross-sections.
- Step 3: In the curvilinear coordinate system, the grid corners (unsampled points) are estimated by any spatial interpolation. To interpolate the data between two cross-sections, it is suggested applying a linear interpolation method along the river (Deltares 2018). Therefore, in this study, in order to maintain continuous wetted areas of the river's interpolated cross-sections, we used a linear interpolation based on a triangulated irregular network (TIN) which derives a bivariate function for each triangle to estimate the depth of unsampled points (Mitas and Mitasova 2005). This accepts the assumption that the riverbed topography has a continuous gradient between adjacent sample points (Sear and Milne 2000). Next the grid corners with estimated elevations in the curvilinear coordinate are converted to the initial Cartesian coordinate system, which is illustrated in Fig. 4. After transforming sample locations in Cartesian coordinates into the curvilinear coordinate, the river topography can be estimated by commonly used spatial interpolation methods. Some interpolation methods were selected to estimate river topographies in the curvilinear coordinate, including linear interpolation, cubic spline interpolation, natural neighbor interpolation, nearest-neighbor interpolation, and IDW. The results are presented in the Appendix.

Calibration of Ordinary Kriging

To carry out an OK interpolation, nugget, sill, range, and model type parameters are empirically defined. This may lead to unexpected errors. To deal with this problem, we combined the Monte Carlo approach with OK interpolation to optimize the selection of uncertain factors. As mentioned previously in the section on OK, the semivariogram function qualifies the spatial correlation of depth samples. From the spatial correlation analysis, the parameters are selected by a fitting empirical semivariogram. Therefore, the Monte Carlo approach is used. This approach will randomly select a value of selected parameters from the semivariogram outputs. The selected parameters are sill, nugget, and range and model type. Fig. 5 depicts the semivariogram model of the interpolated samples. As a result, a fitting Spherical model is empirically defined in which the nugget, partial sill and range are 5, 10, and 8,000, respectively. By applying the Monte Carlo approach, the kriging interpolation is implemented in a large number of 1,000 iterations. The partial sill, nugget, and range are selected in ranges of the model's fitting values adding/subtracting a half of these values. After each iteration, the correlation coefficient was recorded for each interpolated dataset.

Performance Assessment

Cross-validation is commonly conducted to validate spatial interpolation methods (Curtarelli et al. 2015; Zhang et al. 2016). In general, the cross-validation is efficient in the cases where the number of validating samples is much lower than the number of training samples. However, in the situation where the number of validating samples is much larger than the number of training samples, cross-validation is unnecessary.

The performance of the used interpolation methods is assessed by calculating errors that can be presented by statistical indices. There are numerous indicators for determining performance of interpolation methods. The three indices of coefficient of correlation (R), root mean square error (RMSE), and bias are chosen to assess interpolation method performance. Here, R is the degree of relationship between estimation and observation. An R value of 1 is the perfect correlation and indicates that estimation and observation are equal. RMSE is an accuracy measure (Walther and Moore 2005) that is the standard deviation of the interpolation errors. A bias measure used is mean error (ME), which is computed by mean difference between observations and estimates. The R, RMSE, and ME are computed as

$$R = \frac{n\left(\sum s \cdot o\right) - \left(\sum s\right)\left(\sum o\right)}{\sqrt{\left[n\sum s^2 - \left(\sum s\right)^2\right]\left[n\sum o^2 - \left(\sum o\right)^2\right]}} \tag{3}$$

$$\mathrm{RMSE} = \sqrt{\frac{\sum_1^n (s-o)^2}{n}} \tag{4}$$

$$\mathrm{ME} = \bar{s} - \bar{o} \tag{5}$$

where $s =$ is estimation; $o =$ measurement; and $n =$ a number of samples.

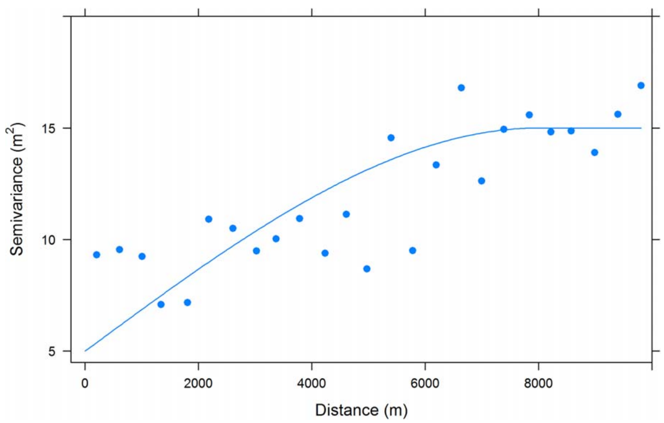

Fig. 5. The cross-section data (points) and the fitting Spherical model (line). The nugget, partial sill, and range are 5, 10, and 8,000, respectively.

Results and Discussion

Calibration of Ordinary Kriging

The results of sensitivity analysis help in understanding the relationship of semivariogram parameters and estimation accuracy and choosing the optimal values of these parameters. Fig. 6 presents the results of sensitivity analysis in which correlations of OK predictions and observations are interpreted by the nugget,

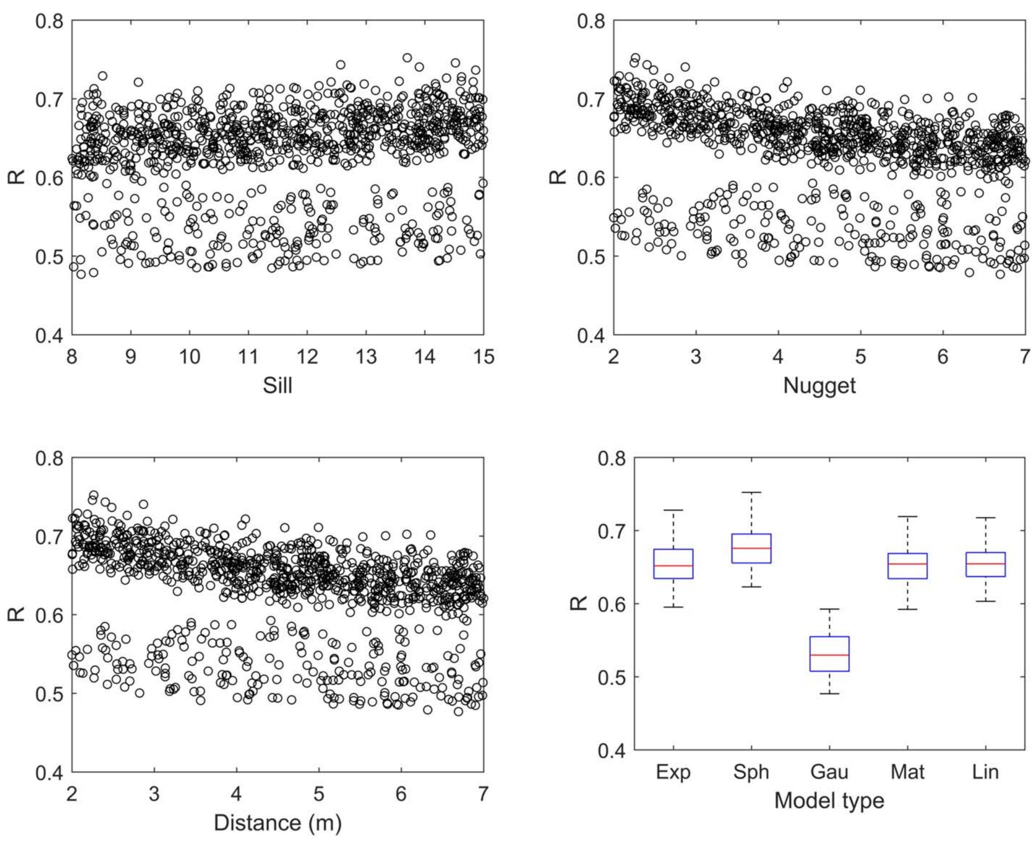

Fig. 6. Sensitivity analysis of semivariogram's parameters.

sill, range, and model type parameters over 1,000 iterations. The OK interpolation method is a stable interpolator which estimates unsampled values in a reasonable agreement with measured data. Here, R values vary in a range from 0.5 to 0.75, and R and nugget inversely relate, but R and partial sill are positively related. Among the parameter sets in sensitivity analysis, the optimal values of nugget and partial sill are 2 and 13 m^2. This sill value of 15 is equal to the values of the empirical fitting curve. It was found that the sill was easily defined when the spatial correlation of data started to level. Nonetheless, the optimal nugget in 1,000 iterations is 2, smaller than that of the empirical fitting curve. Thus when analyzing the data, the nugget parameter is more difficult to define than the sill. As a result of the analysis, the mentioned empirical led to the best R of 0.7 while the optimal R increased to 0.75. In the sensitivity analysis, the random distances were selected from 4,000 to 12,000 m. In fact, when the distances increase, the semivariances increase as well. This means that when pairs of sample points are at a large distance, they have less correlation. Thus the range has a negative relationship with R. The optimal range is 4,250 m. This distance is similar in length to the data for around four cross-sections. It means that riverbed topography is based on the relationship of the data from the four closest cross-sections. In the cases where the samples are uniformly or regularly distributed in space, OK is one of the best interpolators (e.g., Huang et al. 2015). However, spatial distribution of the cross-section data is clumped and riverbed topography is influenced by its flow direction. Thus the OK in Cartesian coordinates is not capable of predicting riverbed surfaces based on limited cross-sectional data. Among the selected model types, interpolators with the spherical model result in the highest R, peaking at 0.75. This indicates that the spherical function is the best fitting model in this analyzing data. Spherical models are commonly chosen for interpolating riverbed topography (e.g., Carter and Shankar 1997; Zhang et al. 2016).

Interpolation of Riverbed Topography

Fig. 7 depicts interpolating results of AR, OK, KED, and IDW interpolating methods compared with the measured data. The riverbed topography generated by the OK method is the worst surface in comparison with measured data. It cannot produce the cross-section shape. For instance, the western segment is a relatively flat bed and the thalweg is not clearly visualized as in the measured data. Therefore, it is not capable of capturing the general trend of riverbed topography. In contrast, the three other methods generated topographies in which the thalweg is reasonably captured. However, prediction errors are different among these methods. The IDW interpolated topography has a slightly discontinuous thalweg and a number of jags. These jags clearly appear in the middle of cross-sections where the values of the riverbed topography are equally affected by the two cross-sections. In order to reduce errors of the discontinuous thalweg problem, the distance-to-thalweg factor of the Kriging with External Drift interpolator (KED) was taken into account. This approach is efficient in generating the thalweg in estimated topography. Nevertheless, this topography has several artificial dunes along the river. These dunes are apparent at shallow cross-sections. This discrepancy may be a result of the geostatistical approach. For riverbed topography, it is better to apply interpolation methods that assume a continuous gradient between sample points of cross-sections. This is determined by the AR interpolated topography. After reducing anisotropy effects, the topography is predicted by the linear interpolation method. The results of the AR interpolation approach have a good agreement with measured data as it is able to capture the continuous thalweg and predict

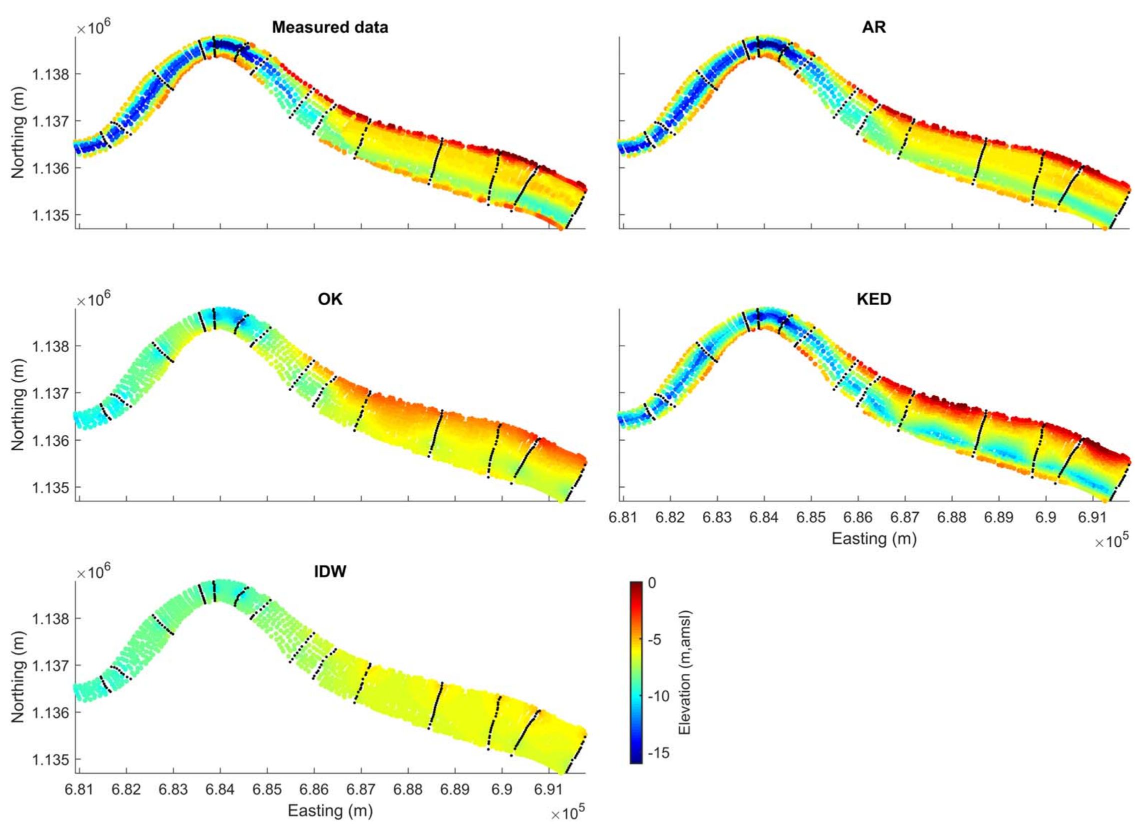

Fig. 7. Riverbed surface estimations of the Cua Tieu branch by different interpolation methods of anisotropy-removed interpolation (AR), ordinary kriging (OK), kriging with external drift (KED), and inverse distance weighting (IDW). The dots are samples which are used for interpolation.

riverbed topography accurately. Nonetheless, there are differences in elevation especially at the southern riverbank. The riverbank elevation is difficult to reproduce because the values of the samples used in interpolating the dataset are not as high as the measured samples. In an application of hydrodynamic modeling, these errors of riverbank elevation are unlikely to influence hydrodynamic results because the riverbanks are usually dry areas. The difficulties of bank elevations can be overcome by adding data from digital terrain models and considering for interpolation.

Interpolation Method Validation

To quantify the accuracies of the applied method, the discrepancies between predictions and measurements are interpreted by the indices of R, RMSE, and ME. Fig. 8 shows scatterplots of predicted and measured topographies and the values of validating indices. The AR method has the highest R of 0.97, followed by IDW, KED, and OK. These R values indicate that the relationship between estimated and measured values have a strong correlation. This determines that the AR method has better performance for simulating variations of riverbed topography. However, R cannot present the difference between predictions and measurements. Thus ME is a common bias measure computed to quantify a system error of these methods. Generally, these methods are good estimators, except for OK. AR, IDW, and KED generate unbiased results, with absolute ME values smaller than 0.1 m, while the ME value of OK is about 0.37 m. RMSE is then used to define accuracy of these predictors. An accurate method should be precise as it predicts unsampled points with small variations. The highest RMSE values of appoximately 2 m are for the OK and IDW estimator. The KED have values of 1.69 m. The smallest variation is generated by the AR method, with a RMSE of 0.74 m. From these validating indices, it can be concluded that the AR method is a good estimator in predicting riverbed topography from cross-section data.

Although the AR is a good estimator, it still has a certain error. To give an insight into further studies, spatial distribution of errors are depicted in Fig. 9. This clearly show that a high frequency of error samples occurs in areas where the river sides and bottom are linked (around 100–200 m from the riverbanks). This holds for all four interpolating methods. The reason for this being that the river in this case has U-shaped cross-sections so elevations in this area are highly variable. Therefore, this characteristic should be noted when defining representative cross-sections for interpolation.

The AR approach includes a combination of three steps and we found that the main step for efficiently generating the river channel topography is coordinate conversion in which samples in Cartesian coordinates are transformed into curvilinear coordinates based on the riverbanks and the thalweg. For instance, the topography of the Tieu branch in the curvilinear coordinate was estimated by some common interpolation methods. The results are shown in Fig. 12 in the Appendix, and have a good agreement with the measured data. These interpolation methods in the curvilinear coordinate generate accurate topographic results. Noticeably, the IDW

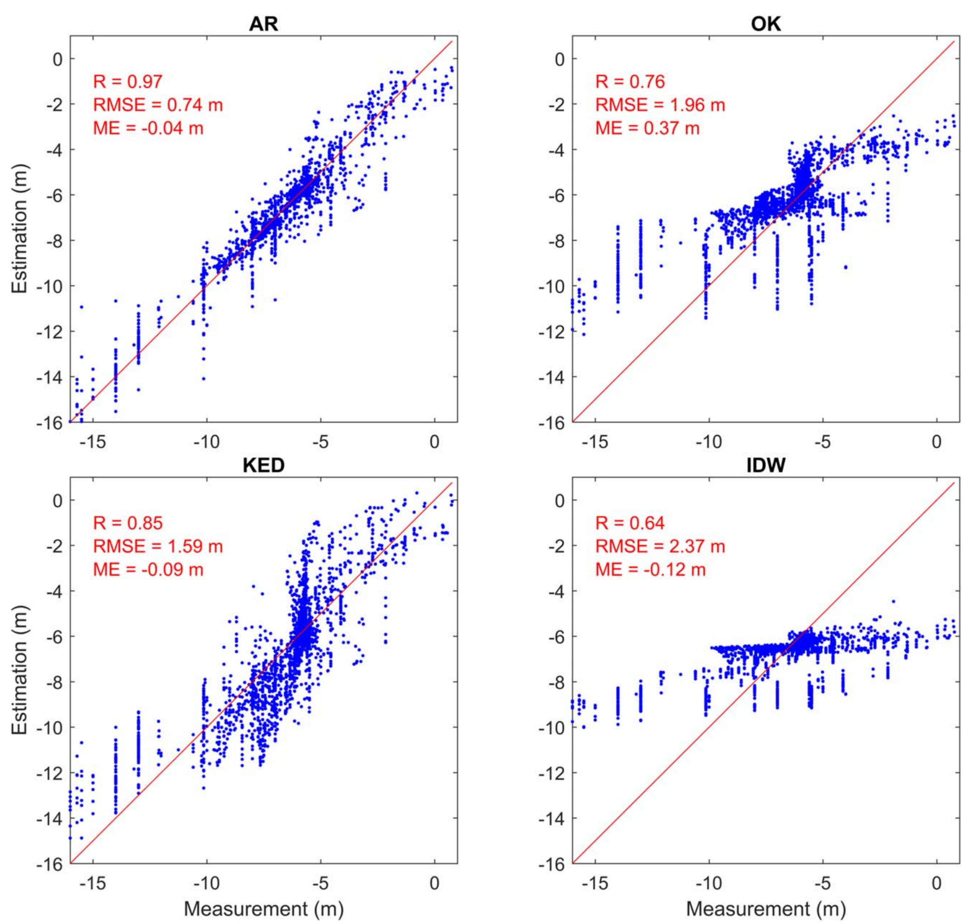

Fig. 8. Scatter plots of depth samples of measurements and predictions by interpolation methods of anisotropy-removed interpolation (AR), ordinary kriging (OK), kriging with external drift (KED) and inverse distance weighting (IDW). Additionally, the performance of these methods are interpreted by indices of coefficient of correlation (R), root mean square error (RMSE), and mean error (ME).

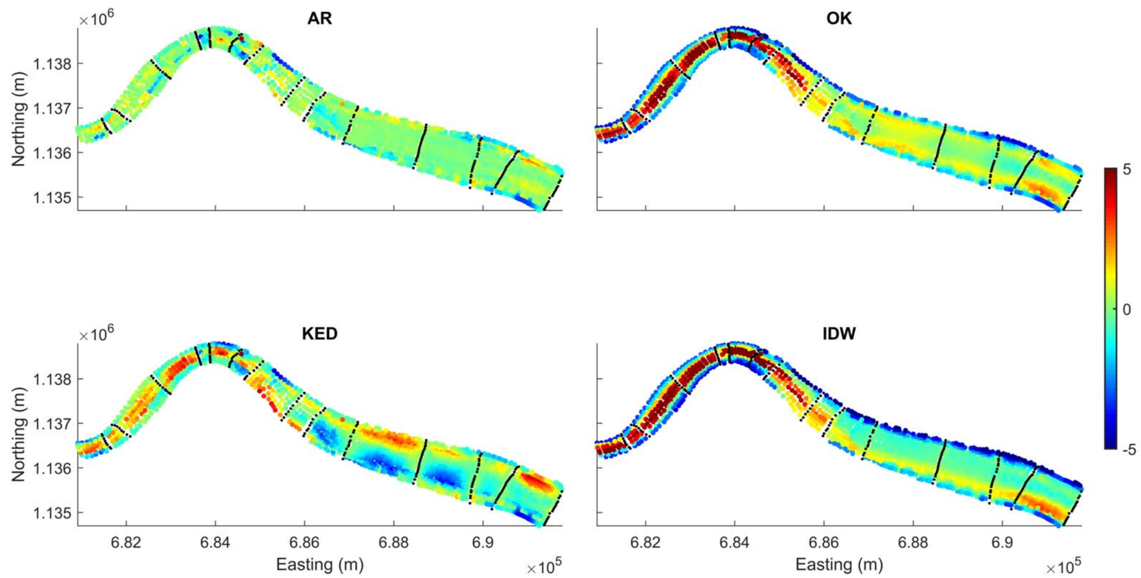

Fig. 9. Spatial distribution of errors generated by interpolators of anisotropy-removed interpolation (AR), ordinary kriging (OK), kriging with external drift (KED), and inverse distance weighting (IDW).

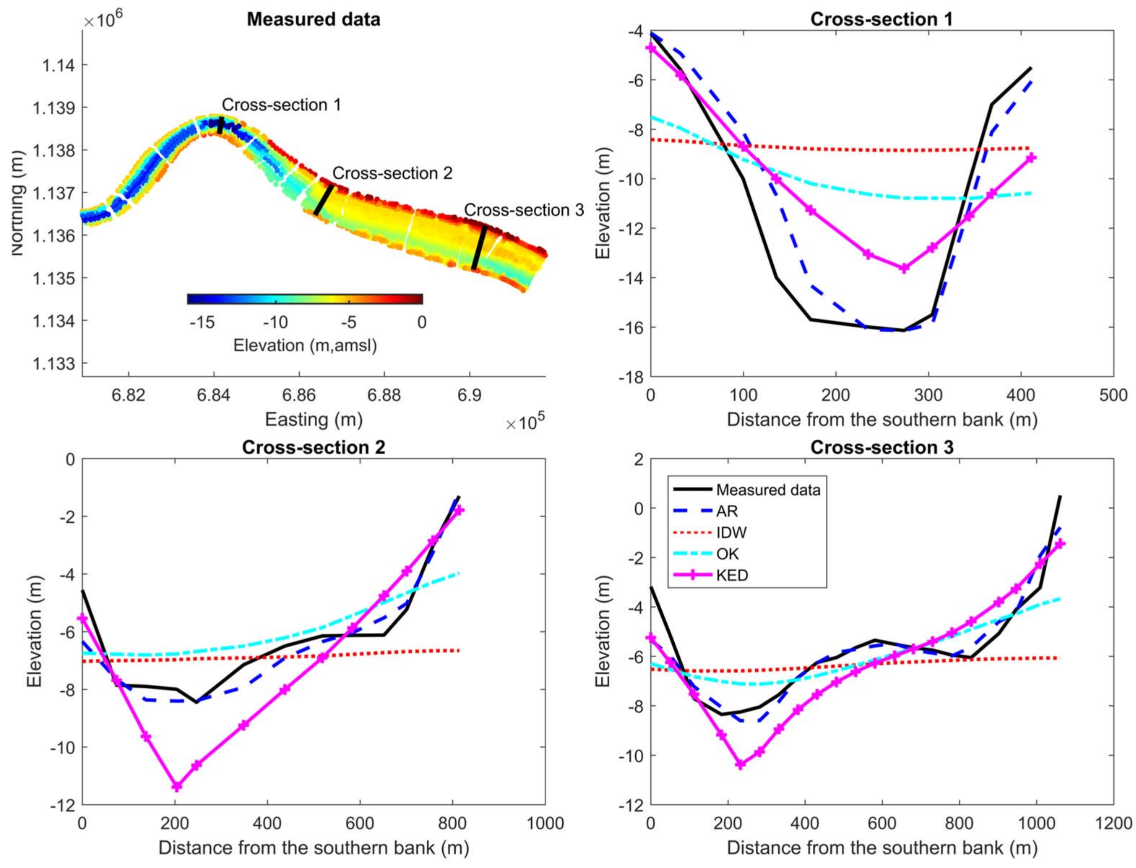

Fig. 10. Measured and interpolated data of the three selected cross-sections.

interpolator in the curvilinear coordinate performs a better topography compared with Catesian coordinates.

Comparison of Cross-Sections and Thalweg Line

Fig. 10 presents measurement and interpolation of the three selected cross-sections. These cross-sections were selected based on river widths, representing narrow, medium, and wide cross-sections. These cross-sections are at the middle of the two adjacent cross-sections used for interpolation, because the middle cross-sections have less influences on these two adjacent cross-sections. In general, the cross-sections reconstructed by using OK and IWD are flat and unrealistic. It clearly shows the effects of the OK and IWD approaches. Specifically, this appeared to be caused by

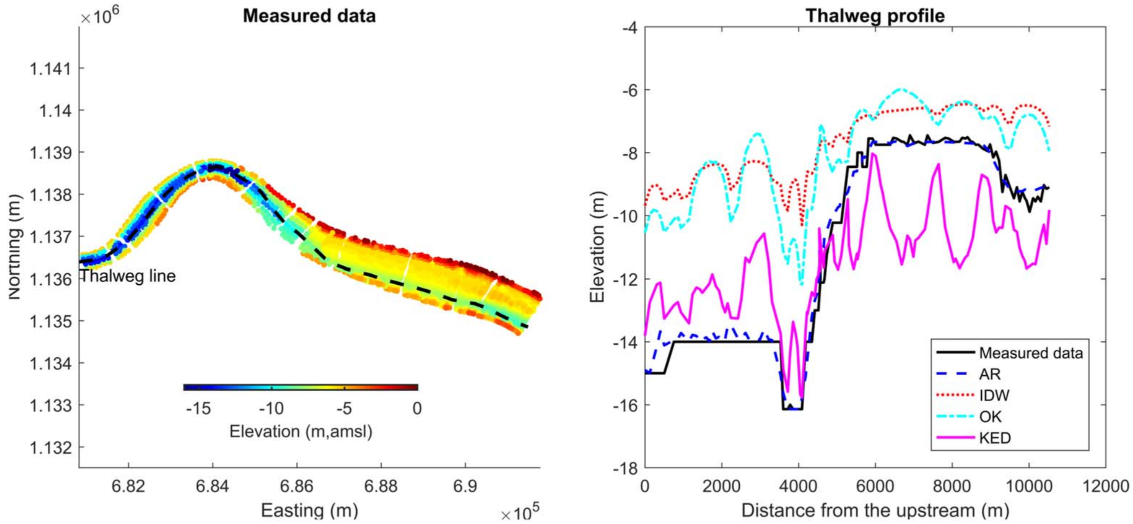

Fig. 11. Measured and interpolated data of the thalweg line.

isotropic approaches for interpolating river topography. In fact, when the directional characteristic of the river topography was considered in the KED interpolation, the cross-section shapes were reproduced. The KED could be capable of reproducing the shapes of cross-sections, but it could generate cross-section elevation precisely (Fig. 10). The AR approach is capable of reconstructing cross-sections shape and elevation accurately. For instance, various morphological singularities of the selected cross-sections were reproduced by using the AR approach. However, there are slight discrepancies between measured and reconstructed elevations. These discrepancies could appear when the samples used for interpolation do not include morphological varations. This should be noted for the field measurement of river topography.

Fig. 11 shows the thalweg profiles of measured data and topography reconstructed by AR, IDW, OK, and KED approaches. The IDW and OK dramatically underestimate thalweg elevations, but they can produce the slope of the bed surface. When considering the thalweg line, the KED also resulted in unsafactory thalweg elevations. Although the KED reasonably generated the thalweg line at the deepest region, it overestimated the fluctuation of the thalweg. This led to nonrealistic dunes and ripples in the interpolated bed surface. The AR approach generated a good fit thalweg. It is able to capture the variations of the riverbed surface. Reconstructing the thalweg line is highly sensitive to cross-sectional inputs. For example, the deepest part is unlikely reproduced if its adjacent cross-sections are used as inputs.

Channel thalweg, as the natural direction of a watercourse, is an important factor to reconstruct river topography. Incorporating the thalweg into the interpolator results in a continuous deepest channel. This makes the bed surface more accurate when reconstructed. We introduced an efficient interpolation approach for generating river bathymetry from sparse cross-sectional data. We also found that the linear interpolation method is better for sparse data regions. However, it is difficult to identify the thalweg line based on sparse data. We suggest generating the thalweg line by connecting splines of the deepest points from cross-section to cross-section. In addition, there are several studies considering the centerline for reconstructing river bathymetry (Goff and Nordfjord 2004; Legleiter and Kyriakidis 2008; Merwade 2009). This could lead to generating a discontinuous thalweg channel. Chen and Liu (2017) used the interpolation methods, namely linear interpolation, IDW, and NN to resample cross-sections and found that the linear interpolation is the most efficient method to reproduce smooth topography and continuous thalweg trajectory.

Conclusions

We proposed an efficient and accurate interpolation approach to be applied for cases of sparse data of river topography. The performance of this method is tested in the sparse data and validated with a high spatial resolution of the Tieu estuarine branch. This approach has better performance in comparison with the commonly used interpolation methods of IDW, OK, and KED. The major difference between these methods is that a channel-fitted coordinate was incorporated, so this is an essential step to reconstruct riverbed topography accurately.

From the results of this study, two major conclusions for interpolating river topographies were drawn. First, excluding anisotropic effects of river topographies should be implemented before applying spatial interpolation methods. Riverbanks and thalwegs are necessary references to diminish the anisotropic effects, especially in meandering rivers. Second, linear interpolation method is one of the best methods to produce river topography from cross-sections. This method generates smooth bed surfaces which are better for hydrodynamic modeling. This study found that reducing anisotropic effects of river channel topography is the main step to reproduce river topography and suggests converting from Cartesian coordinates to the curvilinear coordinate.

The AR approach for generating riverbed topography is helpful in cases of data-poor regions. It is more important when riverbed topography plays a driven role in numerical modeling. Moreover, this approach is crucial for generating the topography of missing data cases. The AR is quite flexible compared with some commercial GIS software. Further work should consist of an extension in order to generate bank elevations from LiDAR data or laser scanning.

Appendix. Comparing Interpolation Methods in the Channel-Fitted Coordinate

In this section the results of some selected interpolation methods were obtained in the transformed coordinate. The theory of these interpolation methods are described by de Boor (2001), Mitas and Mitasova (2005), and Webster and Oliver (2007).

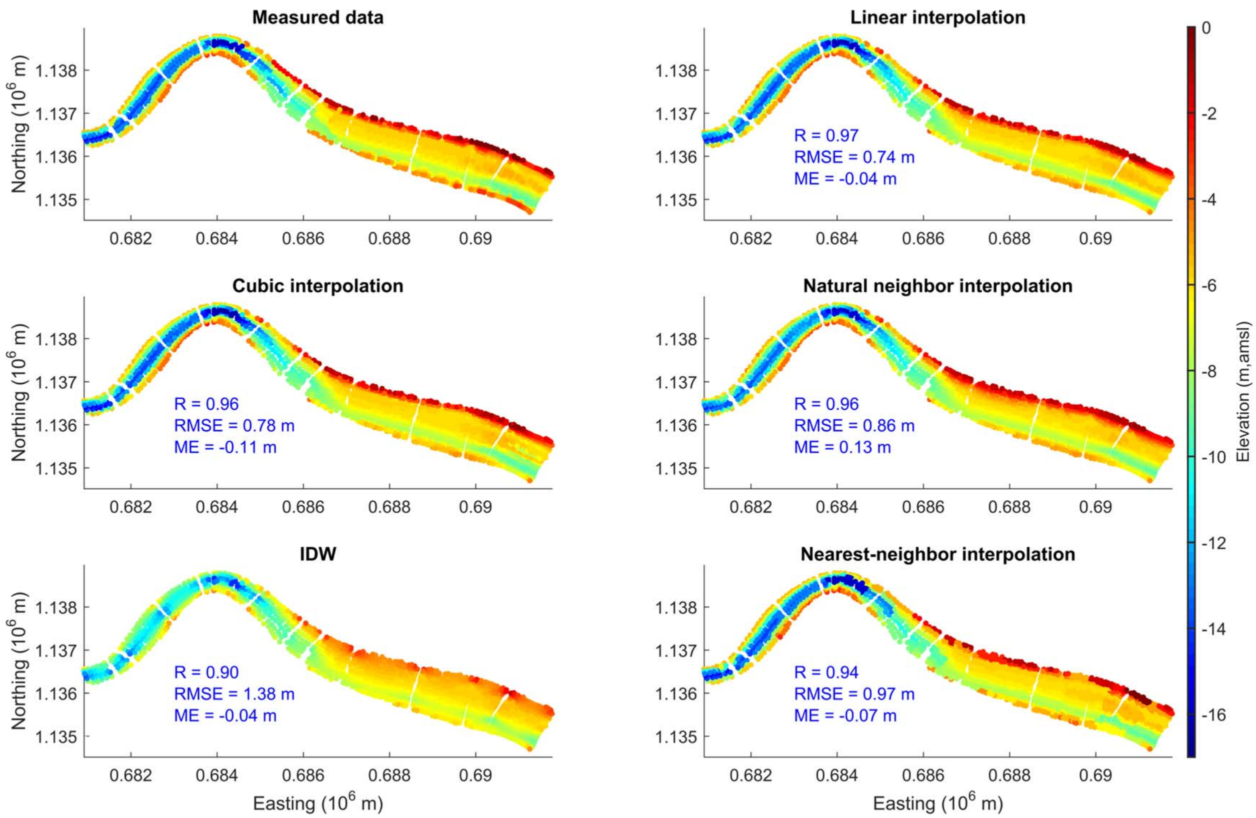

Fig. 12. Topographies of the Tieu branch interpolated by selected methods in the transformed coordinate in comparison with measured data. The interpolated topographies generated by each method are evaluated by statistical indices of correlation (*R*), root mean squared error (RMSE), and mean error (ME).

Data Availability Statement

The data of river bathymetry that supports the findings of this study are not publicly accessible. However, the data and codes can be available from the corresponding author on reasonable request. The curvilinear grid was created by the Delft3D-RGFGRID which is available (https://oss.deltares.nl/web/delft3d/general/subpage1).

Acknowledgments

This project is part of the ONR Tropical Deltas DRI and is funded under grants N00014-12-1-0433 and N00014-15-1-2824.

References

Bailly du Bois, P. 2011. "Automatic calculation of bathymetry for coastal hydrodynamic models." *Comput. Geosci.* 37 (9): 1303–1310. https://doi.org/10.1016/j.cageo.2010.11.018.

Carter, G. S., and U. Shankar. 1997. "Creating rectangular bathymetry grids for environmental numerical modelling of gravel-bed rivers." *Appl. Math. Modell.* 21 (11): 699–708. https://doi.org/10.1016/S0307-904X(97)00094-2.

Caviedes-Voullième, D., M. Morales-Hernández, I. López-Marijuan, and P. García-Navarro. 2014. "Reconstruction of 2D river beds by appropriate interpolation of 1D cross-sectional information for flood simulation." *Environ. Modell. Software* 61: 206–228. https://doi.org/10.1016/j.envsoft.2014.07.016.

Chen, W. B., and W. C. Liu. 2017. "Modeling the influence of river cross-section data on a river stage using a two-dimensional/ three-dimensional hydrodynamic model." *Water* 9 (3): 203. https://doi.org/10.3390/w9030203.

Conner, J. T., and D. Tonina. 2014. "Effect of cross-section interpolated bathymetry on 2D hydrodynamic model results in a large river." *Earth Surf. Processes Landforms* 39 (4): 463–475. https://doi.org/10.1002/esp.3458.

Curtarelli, M., J. Leão, I. Ogashawara, J. Lorenzzetti, and J. Stech. 2015. "Assessment of spatial interpolation methods to map the bathymetry of an Amazonian hydroelectric reservoir to aid in decision making for water management." *ISPRS Int. J. Geo-Inf.* 4 (1): 220–235. https://doi.org/10.3390/ijgi4010220.

de Boor, C. 2001. *A practical guide to splines*. Vol. 27 *Applied mathematical sciences*, edited by J. E. Marsden, and L. Sirovich. New York: Springer.

Deltares. 2018. *D-Flow 1D (SOBEK 3): Hydrodynamics. technical reference manual*. Delft, Netherlands: Deltares.

Dilbone, E., C. J. Legleiter, J. S. Alexander, and B. McElroy. 2018. "Spectrally based bathymetric mapping of a dynamic, sand-bedded channel: Niobrara River, Nebraska, USA." *River Res. Appl.* 34 (5): 430–441. https://doi.org/10.1002/rra.3270.

Dung, N. V., B. Merz, A. Bárdossy, T. D. Thang, and H. Apel. 2011. "Multi-objective automatic calibration of hydrodynamic models utilizing inundation maps and gauge data." *Hydrol. Earth Syst. Sci.* 15 (4): 1339–1354. https://doi.org/10.5194/hess-15-1339-2011.

Goff, J. A., and S. Nordfjord. 2004. "Interpolation of fluvial morphology using channel-oriented coordinate transformation: A case study from the New Jersey Shelf." *Math. Geol.* 36 (6): 643–658. https://doi.org/10.1023/B:MATG.0000039539.84158.cd.

Hilton, J. E., S. Grimaldi, R. C. Z. Cohen, N. Garg, Y. Li, S. Marvanek, V. R. N. Pauwels, and J. P. Walker. 2019. "River reconstruction using a conformal mapping method." *Environ. Modell. Software* 119: 197–213. https://doi.org/10.1016/j.envsoft.2019.06.006.

Huang, C. L., H. W. Wang, and J. L. Hou. 2015. "Estimating spatial distribution of daily snow depth with kriging methods: Combination of

MODIS snow cover area data and ground-based observations." *Cryosphere Discuss.* 9 (5): 4997–5020. https://doi.org/10.5194/tcd-9-4997-2015.
Lai, R., M. Wang, M. Yang, and C. Zhang. 2018. "Method based on the Laplace equations to reconstruct the river terrain for two-dimensional hydrodynamic numerical modeling." *Comput. Geosci.* 111: 26–38. https://doi.org/10.1016/j.cageo.2017.10.006.
Legleiter, C. J. 2013. "Mapping river depth from publicly available aerial images." *River Res. Appl.* 29 (6): 760–780. https://doi.org/10.1002/rra.2560.
Legleiter, C. J., and P. C. Kyriakidis. 2008. "Spatial prediction of river channel topography by kriging." *Earth Surf. Processes Landforms* 33 (6): 841–867. https://doi.org/10.1002/esp.1579.
Li, J., and A. D. Heap. 2011. "A review of comparative studies of spatial interpolation methods in environmental sciences: Performance and impact factors." *Ecol. Inf.* 6 (3–4): 228–241. https://doi.org/10.1016/j.ecoinf.2010.12.003.
Lin, G.-F., and L.-H. Chen. 2004. "A spatial interpolation method based on radial basis function networks incorporating a semivariogram model." *J. Hydrol.* 288 (3–4): 288–298. https://doi.org/10.1016/j.jhydrol.2003.10.008.
Loucks, D. P. 2008. "River models." In *Encyclopedia of ecology*, edited by S. E. Jørgensen, and B. D. Fath, 3069–3083. Amsterdam, Netherlands: Elsevier.
Manh, N. V., N. V. Dung, N. N. Hung, B. Merz, and H. Apel. 2014. "Large-scale suspended sediment transport and deposition in the Mekong Delta." *Hydrol. Earth Syst. Sci.* 18 (8): 3033–3053. https://doi.org/10.5194/hess-18-3033-2014.
Merwade, V. 2009. "Effect of spatial trends on interpolation of river bathymetry." *J. Hydrol.* 371 (1–4): 169–181. https://doi.org/10.1016/j.jhydrol.2009.03.026.
Merwade, V., A. Cook, and J. Coonrod. 2008. "GIS techniques for creating river terrain models for hydrodynamic modeling and flood inundation mapping." *Environ. Modell. Software* 23 (10–11): 1300–1311. https://doi.org/10.1016/j.envsoft.2008.03.005.
Mitas, L., and H. Mitasova. 2005. "Spatial interpolation." In *Geographical information systems: Principles, techniques, management and applications*, edited by P. A. Longley, M. F. Goodchild, D. J. Maguire, and D. W. Rhind, 481–492. Hoboken, NJ: John Wiley & Sons.
Nguyen, A. D. 2008. "Salt intrusion, tides and mixing in multi-channel estuaries." Ph.D. thesis, Dept. of Water Science and Engineering, UNESCO-IHE Institute for Water Education, Delft Univ. of Technology.
Pebesma, E. J. 2004. "Multivariable geostatistics in S: The gstat package." *Comput. Geosci.* 30 (7): 683–691. https://doi.org/10.1016/j.cageo.2004.03.012.
Rivest, M., D. Marcotte, and P. Pasquier. 2008. "Hydraulic head field estimation using kriging with an external drift: A way to consider conceptual model information." *J. Hydrol.* 361 (3–4): 349–361. https://doi.org/10.1016/j.jhydrol.2008.08.006.
Sear, D. A., and J. A. Milne. 2000. "Surface modelling of upland river channel topography and sedimentology using GIS." *Phys. Chem. Earth Part B* 25 (4): 399–406. https://doi.org/10.1016/S1464-1909(00)00033-2.
Thanh, V. Q., J. Reyns, C. Wackerman, E. F. Eidam, and D. Roelvink. 2017. "Modelling suspended sediment dynamics on the subaqueous delta of the Mekong River." *Cont. Shelf Res.* 147: 213–230. https://doi.org/10.1016/j.csr.2017.07.013.
Thanh, V. Q., D. Roelvink, M. van Der Wegen, J. Reyns, H. Kernkamp, G. Van Vinh, and V. T. P. Linh. 2019. *Flooding in the Mekong delta: Impact of dyke systems on downstream hydrodynamics*. Delft, Netherlands: IHE Delft.
Tran, D. D., G. van Halsema, P. J. G. J. Hellegers, L. Phi Hoang, T. Quang Tran, M. Kummu, and F. Ludwig. 2018. "Assessing impacts of dike construction on the flood dynamics of the Mekong Delta." *Hydrol. Earth Syst. Sci. Discuss.* 22 (3): 1875–1896. https://doi.org/10.5194/hess-22-1875-2018.
Triet, N. V. K., N. V. Dung, H. Fujii, M. Kummu, B. Merz, and H. Apel. 2017. "Has dyke development in the Vietnamese Mekong Delta shifted flood hazard downstream?" *Hydrol. Earth Syst. Sci.* 21 (8): 3991–4010. https://doi.org/10.5194/hess-21-3991-2017.
Van, P. D. T., I. Popescu, A. Van Griensven, D. P. Solomatine, N. H. Trung, and A. Green. 2012. "A study of the climate change impacts on fluvial flood propagation in the Vietnamese Mekong Delta." *Hydrol. Earth Syst. Sci.* 16 (12): 4637–4649. https://doi.org/10.5194/hess-16-4637-2012.
Walther, B. A., and J. L. Moore. 2005. "The concepts of bias, precision and accuracy, and their use in testing the performance of species richness estimators, with a literature review of estimator performance." *Ecography* 28 (6): 815–829. https://doi.org/10.1111/j.2005.0906-7590.04112.x.
Wassmann, R., N. X. Hien, C. T. Hoanh, and T. P. Tuong. 2004. "Sea level rise affecting the Vietnamese Mekong Delta: Water elevation in the flood season and implications for rice production." *Clim. Change* 66 (1–2): 89–107. https://doi.org/10.1023/B:CLIM.0000043144.69736.b7.
Webster, R., and M. A. Oliver. 2007. *Geostatistics for environmental scientists*. Hoboken, NJ: John Wiley & Sons.
Wille, K. 2013. *Development of automated methods to improve surface modeling of river channel geometry and features*. Technical Rep. No. SRH-2013-24. Denver, CO: U.S. Department of the Interior.
Zhang, Y., C. Xian, H. Chen, M. L. Grieneisen, J. Liu, and M. Zhang. 2016. "Spatial interpolation of river channel topography using the shortest temporal distance." *J. Hydrol.* 542: 450–462. https://doi.org/10.1016/j.jhydrol.2016.09.022.